Earthq Eng & Eng Vib (2010) 9: 473-480 **DOI**: 10.1007/s11803-010-0029-x

Generation methodology of isolines of earthquake ground motion

Li Wei† and Li Shanyou‡

Institute of Engineering Mechanics, China Earthquake Administration, Harbin 150080, China

Abstract: Due to limited financial resources and challenging geographical conditions, the number of seismic observation networks in China is still very small and they are not widely distributed. Therefore, the available earthquake records obtained after an earthquake have been limited. In this paper, auto-generation methods to obtain strong motion isolines under different conditions are proposed. To verify the accuracy of these methods, some examples, including application to the 2008 Wenchuan earthquake, are given.

Keywords: isolines; interpolation method; attenuation law; strong motion; observation; networks

1 Introduction

With the development of seismic observation networks, the objective of strong motion observation networks has expanded from providing actual data for near-field seismology and earthquake engineering research, to also providing rapid ground motion reports based on real-time and near real-time data obtained from the network for use in earthquake prevention and disaster reduction (Jin *et al*., 2006; Li *et al*., 2002). Moreover, strong motion observation data are important for earthquake disaster protection, earthquake emergency response, disaster assistance and reconstruction (Li, 2004; Li *et al*., 2003). Earthquake early warning and earthquake emergency control systems based on real-time strong motion observation networks are important components in earthquake prevention and disaster reduction, which have received increased attention in recent years (Zhu *et al*., 2002; Li *et al*., 2004).

The generation model of ground motion isolines provides a basis for seismic risk evaluation and loss estimation. Luo and Pan (2009) indicated that the isoline maps are a combination of data and graphics; spatial distribution of geographical objects and the interrelationship of geographical elements can both be represented by isoline maps. A large number of related studies in this area have been carried out throughout the world (Li *et al*., 2008; Yang and Luo, 2010; Wu *et al*., 2008; Enescu and Enescu, 2005).

Correspondence to: Li Wei, Institute of Engineering Mechanics, China Earthquake Administration, Harbin 150080, China
Tel: +86-451-86652637; Fax: 86-451-86652637
E-mail: liw959@126.com
†PhD Candidate; ‡Professor

Supported by: The Science Foundation of IEM. No.2009B05. The National Key Technology R & D Program.No.2009BAK55B01-02. The Science Foundation of IEM. No.2007B11
Received April 8, 2008; **Accepted** August 30, 2010

In this paper, auto-generation methods for strong motion isolines under different conditions are proposed. Using the limited available earthquake records (bedrock PGAs), the influence range of ground motion and its corresponding attenuation law can be quickly evaluated after an earthquake using mathematical methods, such as statistical analysis, interpolation method, and so on, which may be significant for guiding earthquake preparedness and emergency response efforts.

2 Methodologies for generation of isolines of ground motions

In this paper, the development of auto-generation models of isolines is primarily based on the quantity of ground motion parameters and on-site strong motion data obtained. The isolines can be generated by different methods depending on the existing available data in the following three cases:

(1) Only the ground motion parameters are available. Plot the isolines using the known ground motion parameters, earthquake faulting direction (based on the major orientation of active faults near the epicenter) and ground motion attenuation relationship.

(2) Only limited ground motion parameters and a few strong motion observation data are available. Since the least number of observation points is six, when plotting the isolines using discrete observation data, even if there are more than six observation data, if the spatial distribution of the points is uneven, the isolines may differ greatly from the real ones. Therefore, the ground motion field generation method is proposed, which is based on the theoretical value of ground motion and then corrected by real observation data.

(3) A large number of strong motion observation data are available. If there is enough strong motion observation data and the observation stations are

distributed homogeneously, the acceleration values on the regular grid nodes can be obtained directly by using common interpolation methods (Li, 2006), such as the distance-weighted interpolation method based on the least-square method (Wang, 1989), kriging interpolation method (Demyanov *et al*., 1998; Wang *et al*., 1999), modified quadratic Shepard interpolation method (Bai *et al*., 2002) and the distance-weighted interpolation method (Franke, 1982). The isolines of the ground motion field can then be drawn.

A flowchart of computation is shown as follows (Fig. 1):

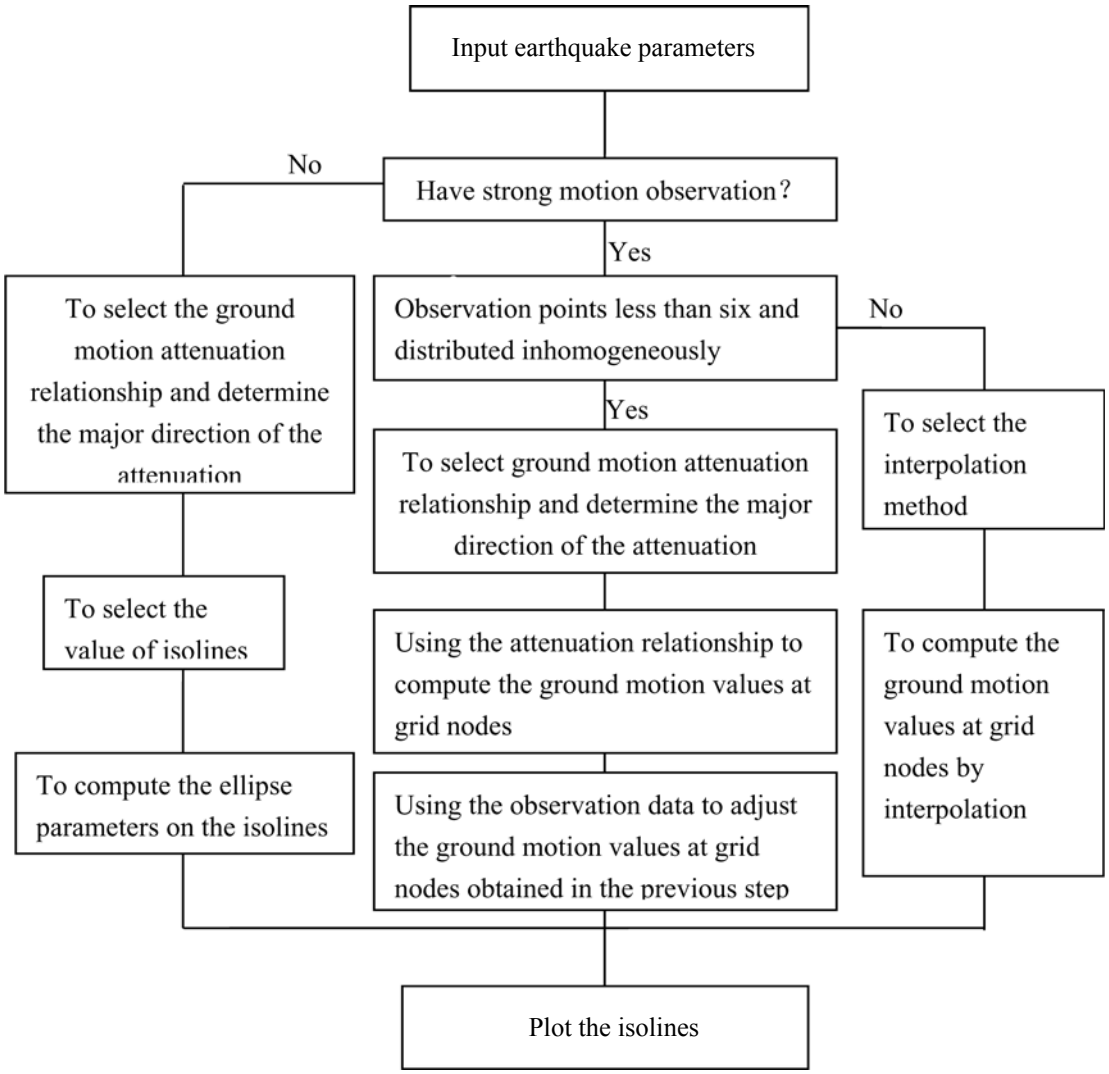

Fig. 1 Flowchart of computation

2.1 Generation of isolines based on ground motion parameters and adequate records

To generate isolines based on ground motion parameters and an adequate number of records, the following steps can be taken.

Step 1: At first, according to the given values of ground motion of the isolines, earthquake magnitude and the ground motion attenuation relationship, the elliptical major axis R_a and minor axis R_b can be identified. Then, plot different isolines of the ellipses along the epicenter and faulting direction.

Step 2: The ground motion values at given grid nodes are computed by using the attenuation relationship and the isolines can be obtained by using the tracing method.

The calculation of the ground motion characteristics values at the grid nodes is as follows: Let the epicenter be the origin of coordinates (0, 0), the angle between the earthquake faulting direction and the horizontal axis x be α; (x_i, y_i) denotes the coordinates of the grid node i. Then, a new Cartesian coordinate system $x'Oy'$ is created, by setting its origin also at the epicenter and its abscissa parallel to the earthquake faulting, (x_i', y_i') denotes the coordinates of the grid node i in the new coordinate system. The following relationship between (x_i, y_i) and (x_i', y_i') can be obtained from the coordinate transformation:

$$x_i^{'} = x_i \cos\alpha + y_i \sin\alpha$$
$$y_i^{'} = y_i \cos\alpha - x_i \sin\alpha \quad (1)$$

For an elliptical function, if the major axis is R_a, the minor axis R_b should be: $R_b = \left|y_i^{'}\right| \Big/ \sqrt{1 - x_i^{'2}/R_a^2}$, R_a increases by 0.1 km pedometer in the interval $\left|x_i^{'}\right|$ to 300 km (suggested values). The values of Y_a and Y_b can be obtained by putting R_a and R_b into the corresponding attenuation formula, then taking the average value of Y_a and Y_b as the ground motion values at the grid nodes when they have the most proximal value.

2.2 Generation of isolines based on ground motion parameters and a few strong earthquake data

The ground motion values are calculated first at the grid nodes by using the attenuation relationship because it requires regular data to generate isolines. The calculation methods are as follows.

(1) Calculate the theoretical values of the ground motion at the grid nodes using the attenuation relationship.

(2) Calculate the ground motion values at the grid nodes near the observation stations again according to the distance-weighted interpolation method and using the real data from the observation station. To employ the function of the real ground motion values from the observation stations, the weight of the real data should be increased.

(3) Use the tracing method to generate the isolines based on the PGAs at the regular grid nodes.

2.3 Generation of isolines based on data from strong ground motion observation network

(1) Directly obtain the PGAs at the regular grid nodes by the generally used interpolation methods, such as the least-square method, kriging interpolationmethod, modified quadratic Shepard interpolation method, distance-weighted interpolation method, etc.

(2) Use the tracing method to generate the isolines based on the PGAs at the regular grid nodes.

3 Examples

The following examples illustrate the generation of isolines using the methods described in Section 2.

It is assumed that the earthquake magnitude is M =7, the angle between the earthquake faulting direction and horizontal direction is 45°, and the ground motion attenuation relationship (GB 18306-2001, 2001) is as follows:

$$\log Y_a = 1.3879 + 0.7413M - 2.3164 \times \log(R_a + 0.7998\exp(0.5299M)) \quad (2)$$

$$\log Y_b = 0.8671 + 0.6136M - 1.8657 \times \log(R_b + 0.6144\exp(0.5299M)) \quad (3)$$

3.1 Generation of the ground motion isolines

3.1.1 Scheme 1

At first, according to the given value of (PGA) of isolines (Y_a, Y_b) , earthquake magnitude M and the ground motion attenuation relationship, the major axis R_a and the minor axis R_b of the ellipse can be identified as listed in Table 1, then the isolines are plotted on R_a and R_b according to the ellipse formula as shown Fig. 2.

3.1.2 Scheme 2

The grid nodes size is set about 10 km×10 km and the Cartesian coordinate system size is set about -100 km to +100 km. The epicenter is set as a grid origin and the angle of the magnitude faulting direction and horizontal direction is 45°. Then the coordinate of grid nodes (x_i, y_i) in the coordinate system of the earthquake faulting direction is generated according to Eq. (1):

Table 1 Ground motion parameters and R_a & R_b of the corresponding ellipses

No.	PGA (Gal)	R_a (km)	R_b (km)
1	500	14.57	17.94
2	400	19.35	20.59
3	300	26.22	24.52
4	250	31.04	27.34
5	200	37.49	31.20
6	150	46.76	36.897
7	100	61.95	46.57
8	50	94.95	68.86
9	25	139.46	101.18
10	10	222.98	167.23

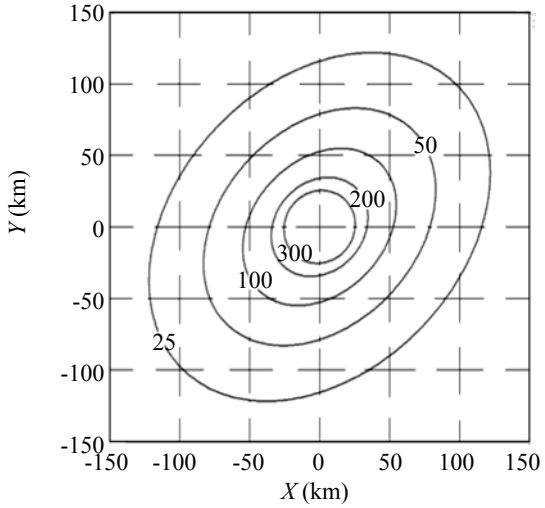

Fig. 2 Isolines of the ellipses generated with given ground motion

$$\begin{cases} x_i^{'} = \sqrt{2}\,(x_i + y_i)/2 \\ y_i^{'} = \sqrt{2}\,(x_i - y_i)/2 \end{cases} \tag{4}$$

(1) When $x_i^{'} = 0$, $y_i^{'} \neq 0$, the grid nodes are located at the minor axis R_b, which is upright to the earthquake faulting direction. In this case $R_b = y_i^{'}$, and the acceleration value can be generated directly using the attenuation relationship of the minor axis.

(2) When $x_i^{'} \neq 0$, $y_i^{'} = 0$, the grid nodes are located at the major axis R_a, which is situated on the magnitude faulting direction. In this case $R_a = x_i^{'}$ and the acceleration value can be generated directly using the attenuation relationship of the major axis.

(3) When $x_i^{'} = 0$, $y_i^{'} = 0$, the grid nodes are located at the epicenter. In this case $R_a = 0$, $R_b = 0$, and the ellipse attenuation relationship can be used directly to generate Y_a and Y_b and their average is taken as the acceleration value.

(4) When $x_i^{'} \neq 0$, $y_i^{'} \neq 0$, the acceleration value at the grid nodes are calculated as follows: According to the elliptical function, if the major axis is R_a the minor axis R_b will be : $R_b = \left|y_i^{'}\right| \Big/ \sqrt{1 - x_i^{'2}/R_a^2}$, R_a increases by 0.1 km pedometer in the interval $\left|x_i^{'}\right|$ to 300 km (suggested values). Calculate the values of Y_a and Y_b by putting R_a and R_b into the corresponding attenuation formula, then take the average value of Y_a and Y_b as the ground motion values at the grid nodes when they have the most proximal value.

Figure 3 shows the isolines obtained based on the grid nodes value.

3.2 Generation of isolines based on ground motion parameters and a few strong earthquake data

Three ground motion values of the observation station are added under a given condition.

The attenuation relationship is used to calculate the theoretical values of the ground motion at the grid nodes (Scheme 2 in Section 3.1.2). Then, re-evaluate the ground motion values at the grid nodes of 60 km×60 km areas in which the three observation stations are centered separately by the distance-weighted interpolation method. To employ the function of the real ground motion values from the observation stations, their weights are increased by 10 times. Then, the isolines are created on the basis of the recalculated grid nodes values.

Figure 4 shows the computation results and the spatial distribution of the stations. The ground motion values and the three selected observation stations are shown in Table. 2.

3.3 Generation of isolines based on the data from strong ground motion observation network

3.3.1 Example 1

If there are enough data of the strong ground motion observation stations and the stations are uniformly distributed, the acceleration values at the regular grid nodes can be directly determined by generally used interpolation methods, such as the least-square method, kriging interpolation method, modified quadratic Shepard

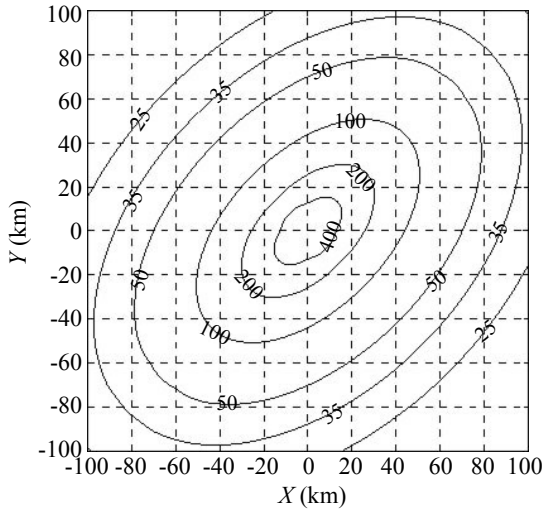

Fig. 3 Isolines charted based on the Scheme 2

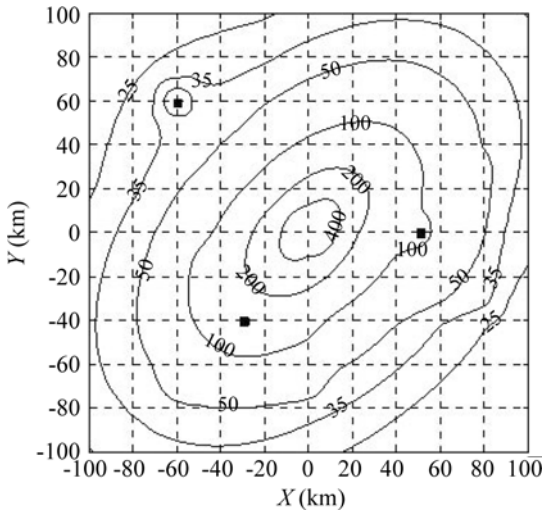

Fig. 4 Isolines charted based on ground motion and few strong motion data

Table 2 Locations of the selected three observation stations and ground motion values

No.	X (km)	Y (km)	PGA (Gal) (Observed value)	PGA (Gal) (Theoretical value)
1	-60	60	77.6	27.6
2	-30	-40	183.1	133.1
3	50	0	132.7	82.7

interpolation method, distance-weighted interpolation method and so on. The isolines can then be plotted. Choose 12 regular data from the results of Scheme 2 in Section 3.1 and use deferent interpolation methods to generate the isolines. (See Table 3, Figs. 5(a)–(d))

3.3.2 Example 2—application to Wenchuan earthquake

After the M8.0 Wenchuan earthquake, a number of strong motion observation data were obtained, and much research work has been carried out (Li *et al*., 2008; Yang and Luo, 2010; Wu *et al*., 2008). In this paper,

Table 3 Coordinates of selected data and corresponding ground motion

No.		1	2	3	4	5	6	7	8	9	10	11	12
Coordinate (km)	X	-60	0	60	-50	70	10	40	-70	-30	80	20	-50
	Y	-80	-60	-70	-50	-20	-10	10	30	30	50	70	80
PGA (Gal)		44.4	63.4	24.3	81.5	39.8	291.3	130.6	35.2	79	47.2	58.5	23.9

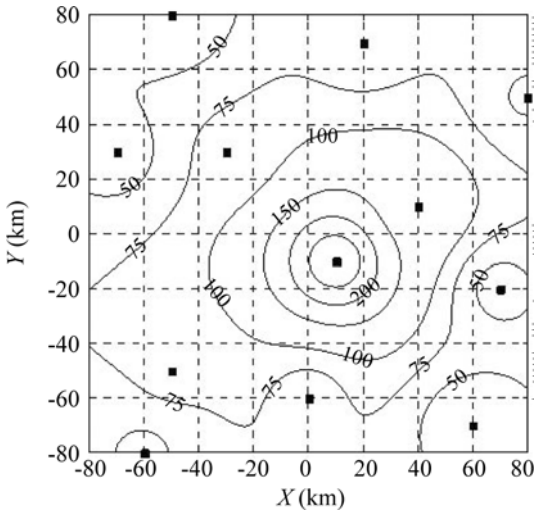

(a) Distance-weighted interpolation

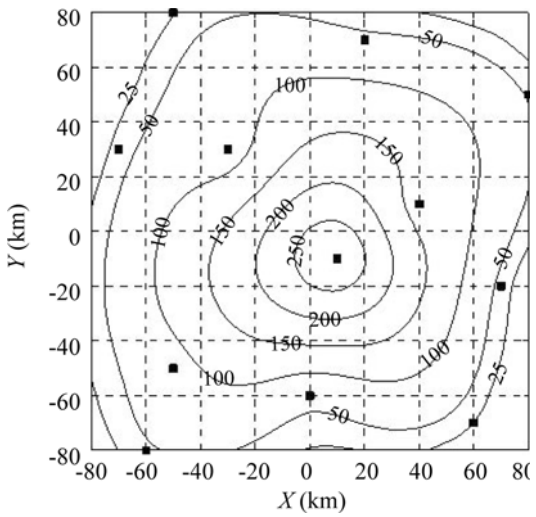

(b) Distance-weighted interpolation based on least-square method

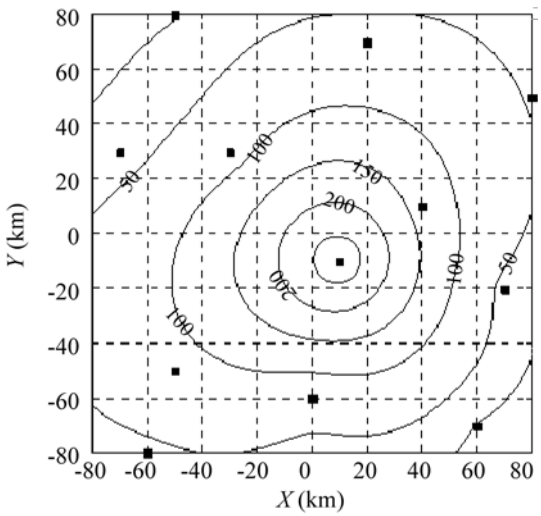

(c) Kriging interpolation

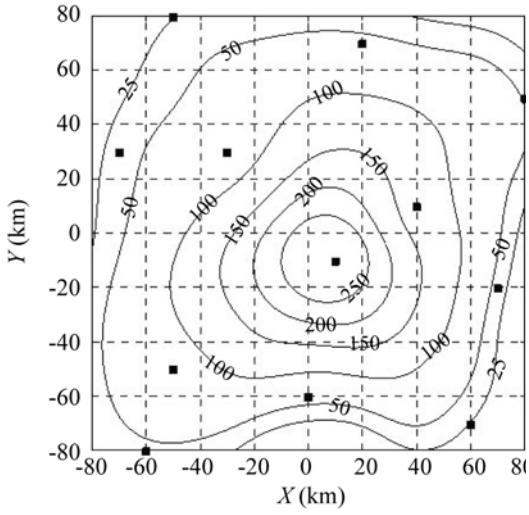

(d) Modified quadratic Shepard interpolation

Fig. 5 Ground motion isolines using different interpolation methods along with spatial distribution of selected data represented by rectangles

Table 4 Coordinates of selected data and corresponding ground motion

No.	Longitude (°)	Latitude (°)	PGA(Gal) (Observed value)	No.	Longitude (°)	Latitude (°)	PGA(Gal) (Observed value)
1	102.34	29.13	103.325	17	102.9	30.54	190.23
2	102.89	29.23	63.221	18	103.18	31.04	957.7
3	102.27	29.28	81.333	19	103.99	31.28	581.592
4	102.44	29.29	85.536	20	104.09	31.52	824.1208
5	102.24	29.43	93.892	21	102.91	31.53	261.755
6	102.62	29.5	83.035	22	103.45	31.56	342.381
7	102.62	29.59	142.3301	23	103.34	31.57	320.938
8	102.99	29.85	102.1007	24	104.74	31.78	511.3302
9	102.87	29.89	117.366	25	104.63	31.78	519.4906
10	103.37	29.91	143.382	26	103.64	32.51	186.5403
11	102.4	29.92	123.282	27	104.21	33.03	173.722
12	102.98	29.99	153.58	28	104.25	33.24	100.041
13	102.92	30.07	124.1405	29	104.11	33.33	112.1909
14	102.93	30.16	118.148	30	104.53	33.66	108.7708
15	103.26	30.42	199.849	31	104.39	34.05	83.964
16	102.88	30.49	153.2508	32	104.02	34.43	70.629

the acceleration values at the regular grid nodes was computed directly by the methods described in Section 3.3.1. The data from 32 observation stations were selected and the isolines were drawn by deferent interpolation methods as shown in Table 4, and Figs. 6 & 7 (a)–(d).

Note that the distribution along the major axis shows good agreement with the actual distribution and the interpolation results are effectively controlled, while the effects of the minor axis are not good. The major reason is that most of the data points are distributed along the major axis of the fault, while fewer points are along the minor axis. Due to the limited actual observation data, it is difficult to conclude which interpolation method is best for the generation of ground motion isolines. However, the Kriging interpolation method appears to be better than others, as it comprehensively considers the influence of various factors.

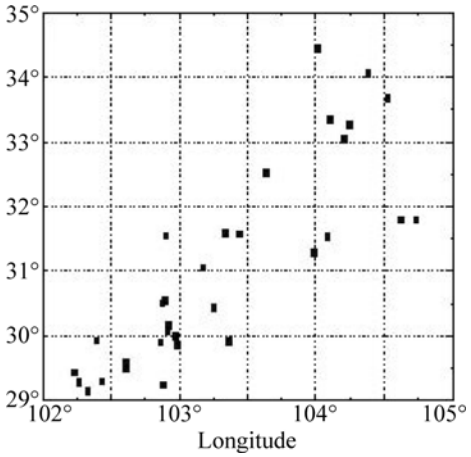

Fig. 6 Spatial distribution of selected data in Wenchuan earthquake

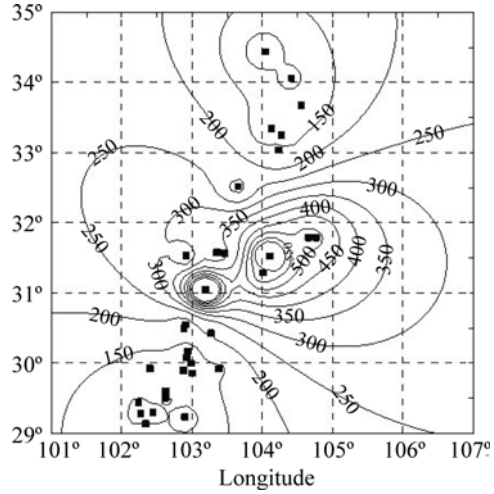

(a) Distance-weighted interpolation method

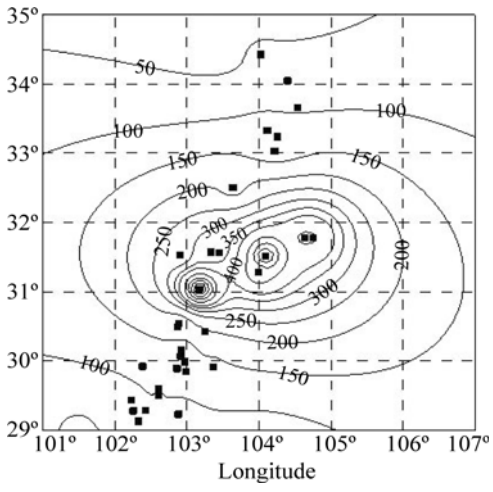

(b) Distance-weighted interpolation based on least-square method

Fig. 7 Ground motion isolines generated by different interpolation methods (the selected data are also shown by rectangles)

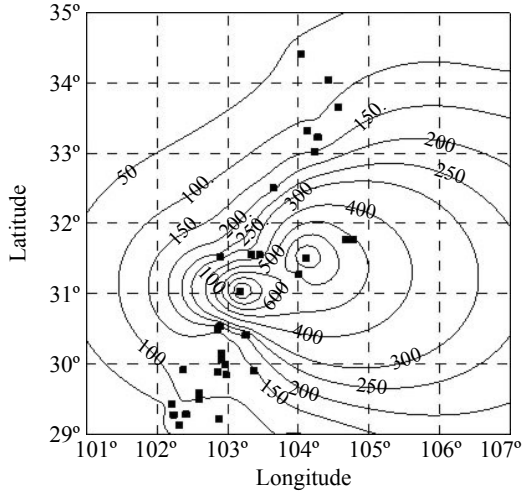

(c) Distance-weighted interpolation

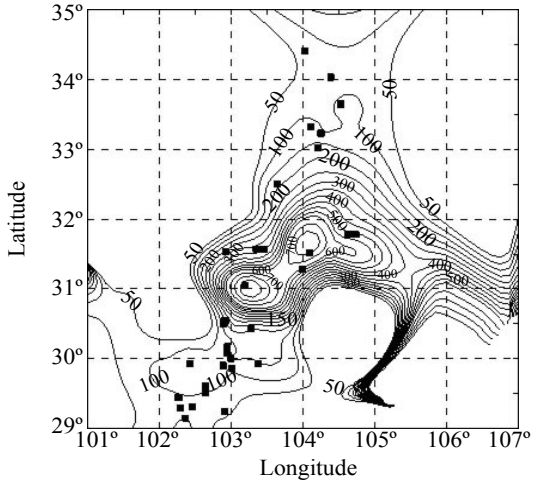

(d) Distance-weighted interpolation based on least-square method

Fig. 7 Continued

4 Concluding remarks

In this paper, the generation methods of ground motion isolines under three different conditions were proposed and their feasibility was verified through examples.

(1) The method based on ground motion parameters and sufficient records can be used when only the earthquake magnitude and the ground motion attenuation relationship can be obtained after an earthquake. Since the attenuation relationships are the empirical statistical equations after previous earthquakes, the isolines computed by using them may not be accurate and can only provide a general estimate of the range of shaking level after an earthquake occurs.

(2) In the method based on ground motion parameters and a few strong motion observation data, the isolines are drawn first by using theoretically computed ground motion values and then modified by the actual observation data.

(3) The method based on data from a strong ground motion observation network draws the isolines directly by using general interpolation methods. The application to the 2008 Wenchuan earthquake found that the distribution along the major axis showed good agreement with the actual distribution and the interpolation results were effectively controlled, while those along the minor axis were not adequate due to fewer data points.

(4) From the examples given in this paper, note that the Kriging interpolation method is preferable, because the influence of various factors is comprehensively considered. For the distance-weighted interpolation method and distance-weighted interpolation based on the least-square method, only the influence of distance is considered; therefore great deviation from the actual results could occur. For the limited actual observation data, the modified quadratic Shepard interpolation method may not provide rational results. However, it is difficult to conclude which of the four interpolation methods is best, and further studies are needed when more actual observation data become available.

References

Bai Shibiao, Chen Ye and Wang Jian (2002), "An Introduction to Nine Gridding Methods and Their Application in Surfer Version 7.0," *Computing Techniques for Geophysical and Geochemical Exploration*, **24**(2): 157–162.

Demyanov V, Kanevsky M, Chernov S, *et al.* (1998), "Neural Networks Residual Kriging Application for Climatic Data," *Journal of Geographic Information and Decision Analysis*, **2**(2): 215–232.

Enescu BD and Enescu D (2005), "Isoline Maps of Ground Motion Acceleration Caused by the Vrancea (Romania) Earthquake of May 30, 1900 (MGR = 6.7) Comparison with the Macroseismic Intensity Map," *Romanian Reports in Physics,* **57**(1):141–150.

Franke R (1982), "Scattered Data Interpolation: Test of Some Methods," *Mathematical Computation*, **38**: 181 –200.

GB18306-2001 (2001), *Seismic Ground Motion Parameter Zoning Map of China* (*2001*), *Western China*.

Jin Xing, LI Shanyou and Li Zuning (2006), "The Prospect of Development and Application of the Earthquake Monitoring Networks," *Earthquake Research in China*, **22**(3): 242–248. (in Chinese)

Li Shanyou (2004), "The Application of Strong Motion Observation," *Seismological Research of Northeast China*, **20**(4): 64–73. (in Chinese)

Li Shanyou, Jin Xing and Liu Qifang (2003), "Prospect of Strong Motion Observation in China," *Earthquake Engineering and Engineering Vibration*, **23**(2): 1–7. (in

Chinese)

Li Shanyou, Jin Xing, Chen Xian and Ma Qiang (2002), "Rapid Reporting of Peak Strong Motion and Seismic Intensity," *Earthquake Engineering and Engineering Vibration*. **22**(6): 1–7. (in Chinese)

Li Shanyou, Jin Xing and Ma Qiang (2004), "Study on Earthquake Early Warning System and Intelligent Emergency Controlling System," *World Earthquake Engineering*. **20**(4): 21–26. (in Chinese)

Li Wei (2006), "The Study on the Rapid Evaluation Method for Seismic Hazard based on the Ground Motion Parameters," *Master Degree Thesis*, Institute of Engineering Mechanics, China Earthquake Administration. (in Chinese)

Li Xiaojun, Zhou Zhenghua, *et al*. (2008), "Strong Motion Observations and Recordings from the Great Wenchuan Earthquake," *Earthquake Engineering and Engineering Vibration,* **7**(3): 235–246.

Luo Xiaoxia and Pan Zhongying (2009), "Isoline Plotting Method of Discrete Geophysical and Geochemical Data," *Second International Symposium on Knowledge Acquisition and Modeling*, Nov. 30–Dec. 01, 2009, Wuhan, China.

Wang Jingbo, Pan Mao and Zhang Xuding (1999), "The Kriging Interpolation Method for Scattered Data Points," *Journal of Computer-aided Design - Computer Graphics*, **11**(6): 525–529. (in Chinese)

Wang Laisheng (1989) *Computer Graphic Processing and its Application of Civil Engineering*, Beijing: Science Press. (in Chinese)

Wu Jian, Lu Hongshan and Liu Aiwen (2008), "Preliminary Study on Correlation between Seismic Intensity and Earthquake Source Process in Wenchuan Earthquake of Sichuan, China," *Technology for Earthquake Disaster Prevention*, **3**(3): 224–229.

Yang Fan and Luo Qifeng (2010), "Wenchuan 8.0 Rank Earthquake Acceleration Peak Attenuation Curve Based on a Four-area Elliptical Model," *Journal of Vibration and Shock*, **29**(5): 136–138.

Zhu Fuxiang, Guo Xun and Li Shanyou (2002), "Preliminary Study on Earthquake Early Warning System for Significant Infrastructure," *World Earthquake Engineering*, **18**(3): 32–36. (in Chinese)